Using a Quantum Equilibrium Ensemble to Uncover the Effects of Cage Flexibility on the Diffusion of Hydrogen Gas in Clathrate Hydrates

Philip Daniel Brous

ABSTRACT

Alternative energy research is turning towards hydrogen as a means of storing renewable energy sources, such as solar energy, and of providing clean fuel to motor vehicles. Storing the gas itself, however, proves to be a difficult task due to the small size of the atoms and low density of the gas. Scientists have expressed interest in clathrate hydrates, crystal lattices of cages made of water molecules, in the past twenty years for their potential to solve the issues of hydrogen storage. The goal is to eventually create a marketable product, but before this can be done, accurate data on clathrate hydrates must be obtained in order to prove their value. Until the cage-to-cage diffusion mechanism of hydrogen gas within the crystal lattice is fully understood, such data cannot be obtained. The flexibility of the clathrate cages has been theorized to play a role in diffusion, but this has yet to be verified numerically. This study seeks to answer this problem and provide some direction for the future of clathrate research. Using the theory of driven adiabatic free energy dynamics, programs were written to obtain the free energy profile for diffusion at several temperatures, assuming rigid cages. Using quantum transition state theory, rates were also obtained. Observation of the differences between the results of this study and a prior study, which obtained the same results but with flexible cages, led to the conclusion that flexibility does indeed play a role in diffusion. This indicates that scientists must take into account flexibility as a factor in future simulations.

1 Introduction

1.1 Background / Significance

1.1.1 The Problems with Fossil Fuels

For years, the scientific community has been focusing its attention on alternative sources of energy because fossil fuels, the main method of energy production for the 20th century, have proven to be both unsustainable and harmful to the environment.[1]

"Unsustainable" refers to the fact that Earth has a limited supply of fossil fuels, and thus in time, the supply will level off, yet the demand will continue increasing.<need ref> Since they are mined from the Earth's crust, and the Earth does not naturally produce them fast enough to keep up with global energy demand, if society continues to mine them at the same rate, it will eventually run out. Economists have coined the event at which oil production slows to a halt the "peak oil phenomenon," and this event is theorized to be a disaster for the world economy.[2] The only way to prevent this catastrophic event would be to continue to expand alternative energy production.[3]

In addition to the fact that it is unsustainable, the byproducts of fossil fuel production have been proven to cause climate change. Not only does this include a rise in temperature, which will melt ice caps and cause a rise in sea levels, covering up towns and cities built on low-altitude dry land, but it includes drastic and dangerous changes in weather patterns. Heavier rainfall will increase the frequency of floods, especially in areas that already see high levels of rainfall. Hotter heat waves will increase the frequency of droughts, threatening to destroy agricultural systems which are crucial to providing food to people. More intense and more frequent hurricanes will ravage towns and cities all over the world.[4]

On top of that, air pollution caused by fossil fuel byproducts will continue to spread respiratory ailments throughout populations in big cities. SO_2 and nitrogen oxides have been directly linked to asthma, bronchitis, and other respiratory diseases,[5] and the burning of fossil fuels is the main source of these substances.[6,7] Additionally, nitrogen oxides cause acid rain, which is harmful for fish, trees, and forest ecosystems in general.[8] China, as an example, is already facing the adverse effects of the burning of fossil fuels; in 2016, the number of deaths attributed to fine particulate matter (soot particles less than 2.5 μm in diameter) climbed above one million.[9] While some scientists look towards technology which can reduce pollution in the atmosphere, given the other effects of fossil fuel production, and the fact that it is unsustainable, it is of much higher importance that scientists develop methods and systems to reduce fossil fuel production altogether.[1]

1.1.2 Alternative Energy Today

Many alternative sources of energy are currently in use today. Nuclear power plants generate energy through nuclear fission reactions, which is efficient and produces no air pollutant byproducts. Solar energy providers are increasing in number, and countries are looking towards other means of energy production, such as wind power. Despite all these advances, however, they all have their own setbacks which prevent them from being expanded.

Nuclear energy, while providing clean energy efficiently, is inherently dangerous. The plutonium byproduct of nuclear energy production is highly radioactive, making it extremely harmful,[10] and by 2000, the nuclear industry had already created 201,000 tons of it.[11] Theoretically, it could be utilized to produce more energy, but the technology for that has yet to be invented. That means that it either has to be stored or turned into nuclear weapons. A 2003 MIT study projected that, if the world expands its nuclear energy production to 1,000 gigawatts by 2050 (an increase of 2% per year), a new Yucca Mountain-sized permanent storage facility would need to be created about every 3 to 4 years to store the extra waste.[11] To make matters worse, it's estimated that nuclear waste must be safely and securely stored for 10,000 to 240,000 years in order to prevent health and environmental disasters from radioactive contamination. Wastes have so far been dumped directly into the ground or into lakes in oceans, but if that continues, it could seriously harm the environment.[11] Lastly, nuclear accidents that occurred in Fukushima and Chernobyl have raised additional concerns about the safety of nuclear energy. These power plant explosions illustrate that a small failure can cause entire cities to fall into a zone of harmful radiation. For these reasons, recent implementation of nuclear power plants has been slow and under heavy debate.[12] Until the problems of nuclear energy are solved, it will remain both a nuisance and a public health hazard, making it a less favorable alternative to fossil fuels.

1.1.3 Why Society Needs Hydrogen Fuel

Another alternative, renewable energy sources, seems to be the future of energy production. States have mandates to increase renewable energy across the board, especially solar energy.[13] Additionally, studies have shown that software systems can be utilized to manage several smaller energy providers in renewable energy, creating a decentralized system of "virtual power plants."[14] However, the main problem that renewable energy sources face is storage. There are many methods by which solar energy can be stored, but one of the most plausible is by the means of hydrogen gas.

Hydrogen gas, or H_2, can be produced straight from water, the most abundant resource on the planet. In addition, with the advent of fuel cell technology, H_2 can be combined with O_2 from the air to produce electricity, heat, and water.[15] Obtaining H_2 from water using electrolysis, the reverse reaction of a fuel cell,

requires more energy to be put into the reaction than it produces, making it inefficient. However, studies have shown that by the means of a photo-catalyst (a material which takes in light energy and converts water into H_2 and O_2), H_2 can be more efficiently produced. Some methods use purified water,[16] and other methods can produce H_2 directly from seawater.[17] With the advent of these technologies, solar energy can be stored in H_2, which can then be cleanly and efficiently converted into usable energy by the means of fuel cells. The sum of all these processes (H_2 production from renewable sources, H_2 storage, and distribution of H_2 to be converted into usable energy through fuel cells) is referred to as the Hydrogen Economy,[18] and is considered desirable by many scientists for its efficiency, environmental friendliness, and ability to provide energy to the people.

1.1.4 Limiting Factors for Widespread Use of Hydrogen Fuels

Currently, H_2 is stored industrially in the liquid state. This, however, is prohibitively expensive to accomplish on a large scale. Being the smallest molecule, H_2 can easily diffuse through any metal or plastic cage. When the pressure and temperature are adjusted, the atoms in the system will lose kinetic energy, reducing losses of H_2. However, maintaining these thermodynamic conditions will always require some amount of energy. Liquid H_2 in particular has a massive energy consumption; the process of liquefaction combined with the cryogenics needed to maintain the liquid state consume a devastatingly large amount of energy, and at atmospheric pressure, H_2 can only remain in the liquid state at temperatures below 20 K.[19] On the small scale, especially, this energy price tag is unacceptable.

Additionally, liquid H_2 is highly flammable. The National Fire Protection Association (NFPA) gives it a rating of 4, its highest risk rating on the scale.[20] Given its low boiling point (311 K) and flash point (296 K),[21] combustion reactions would be deadly, whether they occur at high or low temperatures. This high flammability requires governments to take an inordinate number of safety precautions when storing H_2.[22] While liquid H_2 is ideal in terms of its environmental friendliness and energy density, it lacks in practicality and safety.

1.1.5 Clathrate Hydrates: the Perfect Alternative Storage Material

Clathrate storage, a relatively new method, is a reasonable alternative to liquid H_2 storage as it solves both problems while still maintaining reasonable energy densities.[23] Clathrate hydrates—sometimes referred to as gas hydrates—are ice-like crystal lattices which consist of cages (known as "clathrates") composed of water molecules held together by hydrogen bonds. Since the cage structure is naturally flame retardant, this storage material is much safer than a simple solid tank. The clathrate cages are further stabilized by the introduction of a "guest" molecule,[24] and since H_2 can stabilize the lattice, scientists are looking towards H_2 hydrates—that is, clathrate hydrates with H_2 guests—as a promising storage material.

While H_2 hydrates may occur naturally, they can only form under conditions of high pressure and low temperature, and may form with impurities. However, their molecular constituents—H_2 and H_2O—are two of the most common and easily obtainable materials on this planet, so it is much more economically feasible to mass produce them. Additionally, despite their high formation pressure, once the clathrates are formed, both the temperature and pressure can be eased towards ambient conditions while still keeping the lattice stable.[25]

Ideally, according to experts[23] and the Department of Energy (DOE) Technical Targets for Onboard Hydrogen Storage for Light-Duty Vehicles,[26] the features any H_2 storage material needs to possess in order to become a marketable product are (1) a high H_2 (or energy) per unit mass ratio (1.8 kWh / kg system), (2) a high H_2 (or energy) per unit volume ratio (1.3 kWh / L system), (3) a synthesis pressure preferably lower than 400 MPa (an estimate for the high end of the compression achievable by a simple compressor), (4) almost ambient pressure and moderate temperature for storage (lower than 1.2 MPa and above 233 K), (5) easy H_2 release, and (6) environmentally friendly byproducts.

According to experts, when it comes to meeting these requirements, clathrates are one of the most promising.[23] The following table summarizes the main differences between clathrate hydrate storage and liquid H_2 storage.

Table 1. Rough comparison of clathrate hydrates and standard storage methods.

Storage Method	Clathrate Hydrates	Liquid H_2 Tanks
Energy per unit mass	Lower	Higher
Energy per unit volume	Lower	Higher
Storage Temperature at 0.1 MPa	77 K	20 K
Safety	Safe (non-flammable)	Dangerous (highly flammable)

1.1.6 The Current Contenders

While clathrate hydrates are probably the best alternative to liquid H_2, it is unclear yet to scientists which type is best. Varieties in the structure of the ice crystal lattice can create somewhat significant differences in the properties of different types of clathrate hydrate. Additionally, the introduction of a second guest molecule can have certain benefits. The following paragraphs will discuss the main contenders.

It is already known that one type of clathrate hydrate, structure two (sII), can be formed at pressures well below 400 MPa (as low as 250 MPa at 249 K).[25] sII clathrate hydrates contain two types of cages, small and

large. If Tetrahydrofuran (THF) is added to the solution during synthesis, it will stabilize the larger cages as a secondary guest molecule, and it will lower the synthesis pressure to around 5 MPa.[27] The downside, however, is that the percent capacity by mass and volume of H_2 is severely reduced, as the molecules can only occupy the small cages. sII clathrate hydrates fit and exceed the DOE's H_2 content per unit mass and volume targets, respectively.[23] Once synthesized, the H_2 sII clathrate hydrates can be maintained with a pressure of as low as 0.1 MPa and a temperature of 77 K.[25] While the temperature would have to be quite low, it can always be adjusted if the pressure is increased—something which can be accomplished here because 0.1 MPa is already approximately atmospheric pressure. Although H_2 release has yet to be fully studied, estimates can help demonstrate the ease of such processes. Since the lattice is kinetically stable until 140 K,[28] H_2 will be released from the cages at a slow rate below this temperature. This means that the temperature of the lattice can be raised to temperatures around and upwards of 140 K to achieve the desired rate of diffusion from the system. When H_2 is not being utilized, however, a lower temperature is still required. As for the last DOE requirement, environmental impact is not an issue, given that the cage material is water.

Other clathrate structures have been proposed, but they all carry their own advantages and disadvantages. At high pressure, a new phase called (C_2) arises, containing greater energy densities both by mass and volume. This, however, sacrifices the pressure required to synthesize and maintain the clathrates.[29] The table below summarizes the benefits of the main clathrate structure types that are of interest to scientists.

Table 2. Comparison of different clathrate storage methods

Clathrate Structure	H_2 sII	H_2/THF sII	H_2 C_2
Energy per unit mass (**kWh**/**kg**)	1.8	< 1.8	3.7
Energy per unit volume (**kWh**/**L**)	1.5	< 1.5	3.5
Synthesis pressure (**MPa**)	< 400	< 5	< 2400
Storage Conditions	0.1 MPa & 77 K	< 0.1 MPa & > 77 K	2400 MPa & 298 K
Ease of H_2 release	Projected to be easy	Projected to be easy	Difficult
Environmentally Friendly?	Yes	Yes	Yes

1.1.7 Barriers for Clathrate Hydrates

Clathrate hydrates pose a feasible method for small-scale H_2 storage, so why are they not being produced today? The main reason is that more evidence is needed. Clathrate technology must undergo rigorous testing

by the Department of Energy (DOE) before it can enter the market. A crucial test is determining the diffusion rates within the material framework, as it directly correlates to the efficiency of the storage and release processes. Until the mechanisms behind diffusion are fully understood, scientists will never have accurate data on or full control over the diffusion rates of H_2.

Since experimentation is difficult at such a small scale, scientists have turned to simulation not only to aid in experiment but also to obtain the diffusion rates directly. In order to produce accurate results, the simulations need to include all of the factors that affect the thermodynamics of the system. However, some elements must be sacrificed in order to make these simulations computationally feasible.

In this study, the simulation method to determine diffusion rates uses quantum rate theory, which requires the calculation of the free energy profile of the diffusion process within the clathrate framework. The implementation of quantum theory has been shown to affect the free energy profile, and thus the rates, making it a necessity in future rate calculations.[27] Although experts believe that flexibility could play a role in the diffusion process,[30] it has not been investigated due to a prior focus on other factors and to differences in what studies take into account. If it does not play a role, cages in future studies can be assumed to be rigid, increasing the computational feasibility of simulation. If it does play a role, flexibility can no longer be ignored.

Due to the limitations of previous methodologies and results, no studies have successfully produced accurate enough data for practical applications. The goal of this study is to answer the question of flexibility, in the hopes that it will provide scientists with a framework for determining accurate diffusion rates, thus allowing for the implementation of clathrate hydrate technology in the future.

1.2 Literature Review / Research Problem

The main reason clathrate hydrates have not yet entered the market is that experts do not yet have a clear understanding of diffusion. It is clear in an intuitive sense that flexibility can be the key to this diffusion; if the cage is highly flexible, it could allow for the H_2 guest molecules to escape more easily, thus increasing diffusion rates. Also, prior studies have found that this may be the case.[30] Scientists would like to control the storage and release mechanisms at will, but if flexibility plays such a large role, it may be crucial to model this flexibility.

Additionally, before the method of clathrate hydrates can become a reality, it must go through rigorous testing to prove that it satisfies all of the requirements set forth by government entities such as the DOE. A major obstacle to reaching this goal is that experimental results are difficult to obtain due to the small scale at which they must be performed. Theoretical methods may be the solution. Simulations have been increasingly

employed in this field to study the aspects of clathrates and obtain data.

The simulation process, however, is difficult since simulating only a single clathrate unit cell (the repeating structure in the lattice) requires heavy computing power—large numbers of computations must be performed on hundreds of atoms at a time.

To address the computational issues, there are existing methods to reduce simulation scale, but they also sacrifice physical accuracy. This, however, does not mean that it is impossible to increase efficiency. If a certain factor requires computational power, and that factor does not play a role, it can be discarded from future simulations, and the accuracy will not be altered drastically. There has been much debate over the importance of certain factors, and experts are unsure in what direction to develop this sub-field. This paper chooses to examine flexibility—the most promising factor at the moment—and the role it plays in diffusion, which will help scientists determine the diffusion rates more efficiently in the future. The following paragraphs will discuss some of the debate surrounding clathrates and the successes and failures of previous studies in the field.

1.2.1 Early Studies on Clathrate Hydrates: Cage Structure, Experiment, and Simulation

Early studies in the area provided intriguing evidence that clathrate hydrates could become a potential H_2 storage medium, but while they gave basic answers to some questions, it was clear that more work needed to be done. The concept of H_2 storage using clathrate hydrates arose after it was discovered that clathrate hydrates could be synthesized at pressures between 180 and 600 MPa and temperatures approaching room temperature.[25] The structure consists of a system of two sizes of cages: small cages, which are dodecahedral $\left(5^{12}\right)$, and have an approximate diameter of 5.02 Å, and large cages, which are hexakaidecahedral $\left(5^{12}6^{4}\right)$, and have an approximate diameter of 6.67 Å[25] (Figure 1 shows two dodecahedral cages adjacent to each other, the same system used in this study). Due to the small size of the cages, the maximum occupancy per cage would be expected to be quite small. The first study to approximate these values used experimental stoichiometric ratios between H_2 and H_2O, finding that the large cages had a maximum of 4 H_2 molecules and the small capped at 2.[25] However, further studies have provided contradictory evidence, and a 2005 study gave more evidence of singly occupied small cages.[31] These contradictions could mean two things: either some of the methods that were used were inaccurate, or the H_2 guest molecules are migrating through cage walls. Either way, these studies indicated that the clathrate hydrate has potential, but there was clearly more to be done, as there is a large difference in energy density between having 1 and 2 guest molecules in each small cage.

Studies soon after provided evidence that H_2 guest migration does in fact occur. One study used chemical models to calculate the energy barrier and rate constants for migration, assuming it was possible. The study

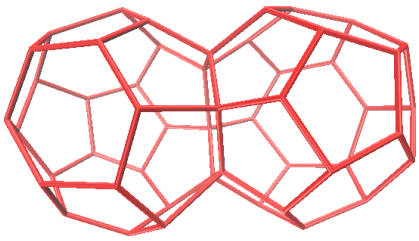

Figure 1. Two large cages connected at a hexagonal face. Hydrogen atoms have been omitted for clarity, and lines between oxygen atoms have been drawn to illustrate the cage structure (created using VMD).

concluded that migration rates would be considerable in the large cages above 100 K and in the small cages above 250 K. It also concluded that quantum tunneling only has an effect below 100 K, so it may be able to be neglected. However, there were many problems with this study. For one, it assumed that everything was rigid, and it found the potential barrier through means of calculating it at only 10 points along the inside of the cage. While it accounted for orientation of the molecule as it approaches the barrier, it failed to explain which orientation would occur.[32] For these reasons, while the study made it fairly certain that cage-to-cage diffusion occurs, the conclusions about quantum effects may have been faulty, and the temperatures at which diffusion becomes important could be questioned.

Another study used an experimental approach to investigate the H_2 dynamics, specifically rotation and, more importantly, cage-to-cage diffusion. Using nuclear magnetic resonance (NMR), a process similar to magnetic resonance imaging (MRI), the study concluded that the patterns arising in the resonance spectra above 120 K (at 1 bar) result from cage-to-cage diffusion of H_2. However, this study only examined ortho-H_2, a particular spin state which only accounts for a small percentage of H_2 present at moderate temperatures.[33] Although it was finally clear after this study that cage-to-cage diffusion occurs, the thermodynamic states at which the guest migration was found to occur were likely inaccurate, and thus further testing was needed.

Among the previous studies, there appeared to be another problem. The molecular simulation studies had found the barriers for cage-to-cage migration to be as high as 118 kJ mol^{-1} between small cages,[32] but experimental studies similar to the one described previously had discovered barriers as low as 3 kJ mol^{-1}.[34,35] The latter value was obtained in the presence of THF as a promoter molecule, but this should not have made a difference, as THF occupies the large cages, so when present, H_2 migration would be expected to happen solely between small cages.[30] Thus, both values represent small cage migration, which presents a contradiction, as the values are starkly different.

1.2.2 More Recent Studies: Developed Simulations and Quantum Effects

A 2015 study attempted to clear up this confusion surrounding free energy data with a detailed look into the dynamics of H_2 migration. Using NVT ensemble simulations in the Ab Initio molecular dynamics package, it took into account several factors, including orientation of the H_2 molecule. This time, instead of simply looking at migration between small or between large cages, it looked at migration between a large and small cage. Also, it repeated these simulations using different occupancies of H_2 and THF in the large cage. In the end, it concluded that the discrepancy in energy values was likely due to a number of things. For one, H_2 guests may use large cages containing THF as a "lane of transport," meaning that guests can migrate into large cages despite the presence of THF. This would mean that the rate of diffusion could increase, which could explain the unusually low potential barrier found when THF was present. Also, increased occupancy of the cages severely lowers the barrier for diffusion, and if the cages can be momentarily filled with more H_2 guests than previously calculated, then diffusion will quickly occur to even out the distribution of molecules. The lowest value obtained by assuming momentary occupation of a large number of guests was 5 kJ mol-1, indicating that this effect is likely to contribute to the low barrier, as it matches closely with the lowest experimental values. Lastly, the study showed that hydrate flexibility may also be part of the explanation. The studies that reported high barriers did not take into account the flexibility of the clathrate, and in this study, the barriers for flexible clathrates were significantly lower.[30] Although the argument that flexibility plays a role originates here, it was far from resolved, as this study failed to account for certain key issues, mainly quantum effects.

Previously, there was good reason to avoid factoring in quantum effects, as they appeared to affect the guest migration only below the temperatures at which clathrate hydrates would likely be stored. However, other evidence suggests that they may be more relevant than previously thought. A 2016 study decided to test the relevancy of these quantum effects. A series of blue moon calculations using path integral molecular dynamics (PIMD) concluded that quantum effects likely play a large role in the free energy profile and diffusion rates at temperatures below 25 K.[27] More recently, a 2017 study used the advent of quantum effects to confirm that the small cages are singly occupied and the large cages contain up to 4 molecules of H_2.[36]

While both of these studies improved on scientists' understanding of diffusion in the system, they both failed to address the issue of flexibility in the clathrates. As was shown in the 2015 study, flexibility possibly plays a large role in the mechanism of diffusion. Intuitively, this makes sense.[30] Flexible cages could allow for the face of the cage at the transition state to expand, allowing for a lower barrier energy. Or, flexibility could end up enclosing the H_2 even further, increasing the free energy profile.

1.2.3 Summary

In summary, while all of these studies have increased scientists knowledge of the clathrate hydrate system, flexibility is an issue that has yet to be addressed. Now that quantum effects have been shown to play a role in diffusion, a study is needed which tests the effects of flexibility when the system is assumed to be quantum. This study provides that test and thus attempts to answer to the question.

1.3 Hypothesis

If the free energy surface for cage-to-cage diffusion for H_2 in the sII clathrate hydrate is obtained while assuming rigidity of the cages, then the data will be significantly different from that obtained by taking into account the flexibility of the cages.

2 Methods

2.1 Molecular Dynamics and the Connection to Path Integrals

Hamiltonian mechanics allows for the total energy of a system of particles to be directly translated into a small number of differential equations that encode the trajectories, otherwise known as the "equations of motion." The total energy is simply a function of the coordinates of each particle in phase space, which refers to the 6N-dimensional space that fully describes a system of N particles. The number 6N comes from the fact that for each particle, there are 3 position components and 3 momentum components being tracked. Molecular dynamics (MD) is the name of the process in which these "equations of motion" are "integrated" to obtain the trajectories of each particle in phase space (in other words, the 6 coordinates of each atom at each time step).

There are a wide range of methods by which the equations of motion can be integrated, all of which fall under the category of MD. Path integral molecular dynamics (PIMD) connects MD to Feynman's path integral formulation of quantum mechanics.[37]

According to the path integral formulation of quantum mechanics, the discrete N-particle partition function, which describes the number of microstates for a given macrostate, is:

$$\begin{aligned} Q_P(N,V,T) = &\prod_{i=1}^{N}\left(\frac{m_i P}{2\pi\beta\hbar^2}\right)^{dP/2}\int\prod_{i=1}^{N}\mathrm{d}\mathbf{r}_i^{(1)}\cdots\mathrm{d}\mathbf{r}_i^{(P)}\mathrm{d}\mathbf{p}_i^{(1)}\cdots\mathrm{d}\mathbf{p}_i^{(P)} \\ &\times\exp\left\{-\beta\sum_{k=1}^{P}\left[\sum_{i=1}^{N}\frac{\mathbf{p}_i^{(k)^2}}{2m_i'}+\sum_{i=1}^{N}\frac{1}{2}m_i\omega_P^2\left(\mathbf{r}_i^{(k+1)}-\mathbf{r}_i^{(k)}\right)^2+\frac{1}{2}U\left(\mathbf{r}_1^{(k)},\ldots,\mathbf{r}_N^{(k)}\right)\right]\right\} \end{aligned} \tag{1}$$

where $\omega_p = \sqrt{P}/(\beta\hbar)$, $m_i' = m_i P/(2\pi\hbar)^2$, the lower indices indicate the atom, and the upper indices indicate the bead number.

These fictitious particles are labeled "beads" since the partition function directly reflects that of a classical partition function for several cyclic polymer chains in which the particles in the chains are coupled to their nearest neighbors harmonically. These chains are commonly referred to as ring polymers, as each ring represents an atom. Since the ring polymer looks like a necklace, the individual particles are called "beads" (see figure 2).

The Hamiltonian, another word for the total energy of the system, is simply the argument of the exponential in eqn. 1 to the right of the $-\beta$. Using Hamiltonian mechanics, the equations of motion can be derived, and, since this partition function is in the canonical ensemble, its equations of motion employ thermostats (see section on d-AFED for more information).

The use of path integrals does allow for the inclusion of quantum effects, but the interpretation of this bead-spring model of atoms can be difficult to interpret. For example, calculating a free energy curve associated with each bead would have no physical interpretation and be tedious. What scientists in this sub-field commonly do is take the centroid of the beads for each atom, which drastically simplifies the calculation and gives the beads a physical representation. This can, however, produce problems, as the centroid is only an approximation of the true behavior of these quantum systems, and the centroid can sometimes veer far off from the beads themselves. In the case of this study, though, the specific collective variable used has minimal error. In all of the following equations, a "c" subscript indicates that the collective variable is tracking the centroid of the beads for each atom.

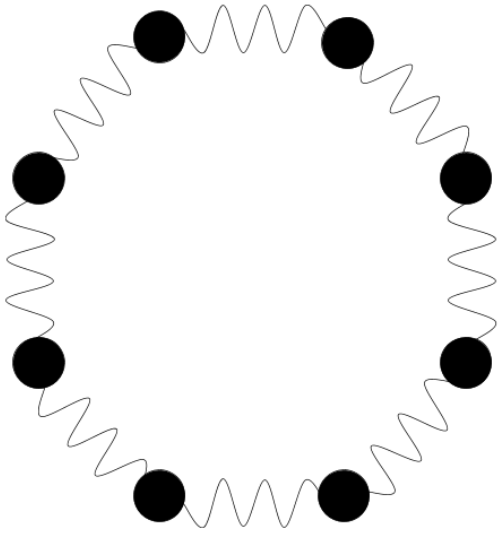

Figure 2. The bead-spring model of an atom. Each spring represents a harmonic coupling and each ball represents a bead.

2.2 Driven Adiabatic Free Energy Dynamics (d-AFED)

In statistical mechanics, it is commonplace to use a "collective variable" (CV), which is a function of the coordinates. For an N particle system, the CV is represented as $q(\mathbf{r}_1, ..., \mathbf{r}_N)$, or $q(\mathbf{r})$ in shorthand. In chemical simulations, without specification of a CV, the sampling will occur at random points in the accessible phase space of the system. This is unfavorable, as the points which the scientist wants to study may be missed in the sampling. The purpose of selecting a CV or set of CVs is to be able to restrict sampling to a certain specified "slice" or region of phase space.

Restricting the phase space, however, doesn't solve all sampling problems. When standard techniques are employed to sample free energies, for example, one will often run into "rare event" problems. In the canonical ensemble, the probability that a CV will sample a configuration of phase space whose potential energy is U_{top} at the top of a barrier is proportional to $\exp[-U_{top}/kT]$. This means that when $kT << U_{top}$, the probability of barrier crossing—which is necessary in many cases to sample the full phase space—is inadequately low. This is what is referred to as a "rare event" problem. Increasing the temperature may increase this probability, but it would also end up broadening the ensemble distribution, thus changing the thermodynamics of the system.

An enhanced sampling method which attempts to solve the problem of "rare events," driven adiabatic free energy dynamics, or d-AFED,[38,39] gets its name from the idea that it physically drags (or drives) the system over the barrier. It does this by harmonically coupling a virtual particle to each of the CVs of interest. The Hamiltonian of the system will look like:

$$\tilde{\mathcal{H}}(\mathbf{r}, \mathbf{p}, s, p) = \mathcal{H}(\mathbf{r}, \mathbf{p}) + \sum_{\alpha=1}^{n} \left[\frac{p_\alpha^2}{2\mu_\alpha} + \frac{1}{2} \kappa_\alpha \left(q_\alpha(\mathbf{r}) - s_\alpha \right)^2 \right], \tag{2}$$

where $q_\alpha(\mathbf{r})$ is the CV, κ_α is the coupling constant for each $q_\alpha(\mathbf{r})$, and p_α & μ_α are the momentum and mass of each virtual particle, respectively. The virtual particle allows the temperature to be raised indefinitely without interfering with the ensemble distribution. It achieves this through an adiabatic decoupling in which μ_α is raised much higher than the mass of any physical particle.

Given that d-AFED operates within the canonical ensemble, and the microcanonical ensemble distribution is more useful for free energy calculations, thermostats must be employed. Thermostats are simply extra terms added onto the Hamiltonian in order to maintain a relatively constant temperature. The following equations are rough representations of the actual equations of motion (each $\mathbf{r}_i$ tracks a physical atom, and T_s is the temperature of the virtual particle):

$$m_i\ddot{\mathbf{r}}_i = -\nabla_i U(\mathbf{r}) - \sum_{\alpha=1}^{n} \left[\kappa_\alpha \left(q_\alpha(\mathbf{r}) - s_\alpha\right) \nabla_i q_\alpha(\mathbf{r})\right] + \text{thermostat}(T)$$

$$\mu_\alpha \ddot{s}_\alpha = \kappa_\alpha \left(q_\alpha(\mathbf{r}) - s_\alpha\right) + \text{thermostat}(T_s) \tag{3}$$

Once the coordinates are obtained, the mean force can be calculated by the following equation:

$$F_\alpha(s) = \left\langle \kappa_\alpha \left(q_\alpha(\mathbf{r}) - s_\alpha\right)\right\rangle = -\frac{\partial A}{\partial s_\alpha}, \tag{4}$$

In the simulation, this entails constructing a histogram of the CV and taking the average in each bin. These forces can then be integrated according to the following equation in order to obtain the Helmholtz free energy surface:

$$A(s_1, ..., s_\alpha) = -\int \prod_{\alpha=1}^{n} F_\alpha(s) \mathrm{d}s_\alpha \tag{5}$$

2.3 Quantum Transition State Theory (QTST)

In quantum transition state theory, the (static) rate of diffusion through the transition state in a quantum system can be calculated using the following equation:

$$k_{\text{QTST}} = \frac{1}{\sqrt{2\pi\beta\mu}} P(q_c^\ddagger), \tag{6}$$

where $\beta = 1/(k_B T)$, μ is the reduced mass of the system, and $P(q_c^\ddagger)$ is the probability per unit length of finding reaction coordinate q at the transition state $q_c^\ddagger$. This probability is calculated by the following equation:

$$P(q_c^\ddagger) = \frac{e^{-\beta A(q_c^\ddagger)}}{\int_{q_0}^{q^\ddagger} e^{-\beta A(q_c)} \mathrm{d}q_c} \tag{7}$$

The Eyring–Polanyi equation describes the temperature dependence of k_{QTST}, which allows for graphs of rates versus temperature to be linear ($\Delta^\ddagger A^\Theta$ is the activation energy):

$$\ln(k_{\text{QTST}}) = -\frac{\Delta^\ddagger A^\Theta}{R} \cdot \frac{1}{T} + \ln\left(\frac{k_B T}{h}\right) \tag{8}$$

2.4 Computational Details

The computational steps taken throughout the methodology in chronological order are summarized in figure 3, and the rest of this subsection goes into detail on these methods and their parameters:.

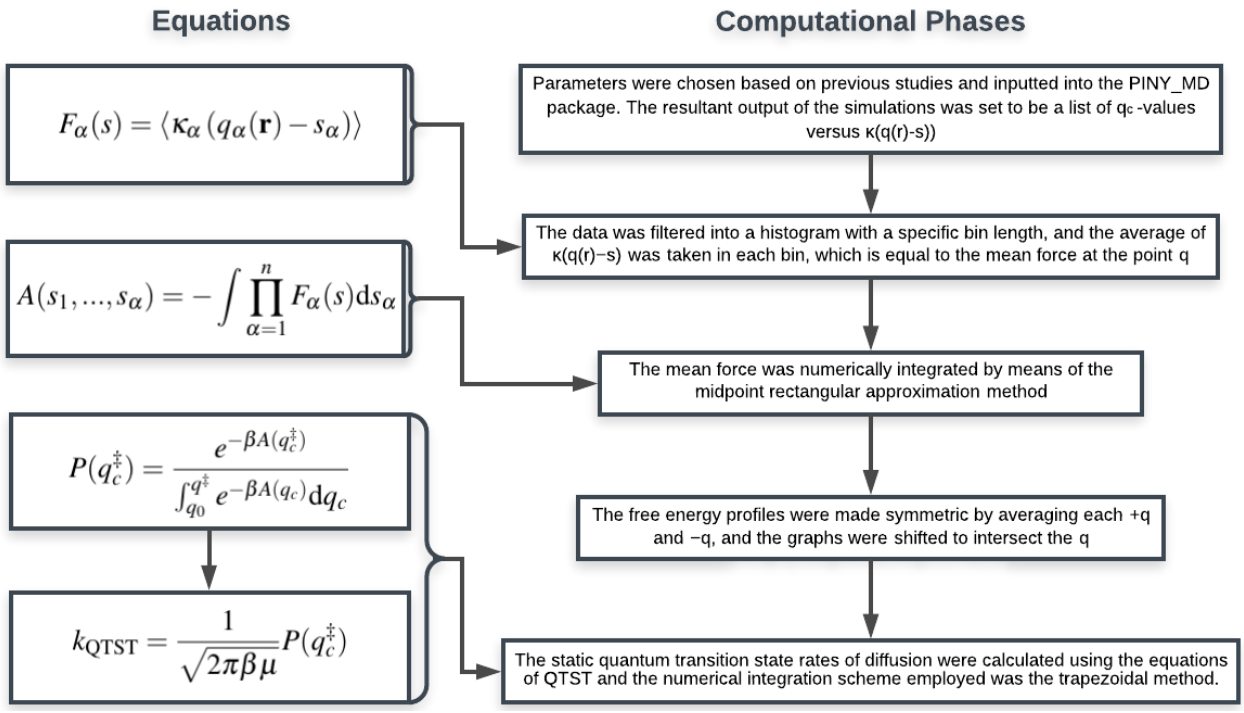

Figure 3. A summary of the computational steps of the methodology with the equations each step incorporates

This study examines only a single CV, as the free energy profile of diffusion is best described by a one-dimensional reaction coordinate. Thus, only one virtual particle was necessary to drive the reaction. The CV was defined as follows:

$$q_c(\mathbf{r}_c) = \left[\frac{1}{2}\left(\mathbf{r}_c^{H_a} + \mathbf{r}_c^{H_b}\right) - \mathbf{R}_A\right] \cdot \hat{\mu}_{AB} - \frac{|\mathbf{R}_B - \mathbf{R}_A|}{2} \tag{9}$$

Each $\mathbf{r}_c$ represents the centroid for each ring polymer hydrogen atom, $\frac{1}{2}\left(\mathbf{r}_c^{H_a} + \mathbf{r}_c^{H_b}\right)$ represents the center of mass of H_2, $\mathbf{R}_A$ and $\mathbf{R}_B$ represent the center of mass of cages A and B respectively, and $\hat{\mu}_{AB} = \frac{\|\mathbf{R}_B - \mathbf{R}_A\|}{\mathbf{R}_B - \mathbf{R}_A}$. This specific formula was chosen based on previous studies and on the fact that it gives a full picture of the diffusion reaction. At the transition state, the point halfway in between the cage centers, $q_c(\mathbf{r}) = 0$. Thus, the sign of the CV indicates the cage in which it is located.

To make the cages rigid, a constraint was imposed on each cage atom which applies an opposing force at each time step. Since the net force is zero, the cages are "frozen" in place. The thermostat methods used were Nosé Hoover chains[40] for the physical particles and the isokinetic approach[41] for the virtual particle. The velocity Verlet algorithm was used to integrate the equations of motion.

These techniques were implemented in several PIMD simulations by the PINY_MD package.[42] The number of beads used for each temperature were 4 for 200 K, 8 for 100 K, 16 for 50 K, and 32 for 25

K. Higher bead numbers were used for lower temperatures since the role of quantum effects increases as temperature decreases. Once the coordinates were obtained, PINY_MD calculated and outputted $\kappa(q_c(\mathbf{r}) - s)$ for each value of q_c sampled.

Simulations were run with a time step of 0.25 fs, and the total simulation time was 500 ps. The coupling constant κ was set as 1.0 hartree $\cdot$ Å^{-2} and the mass and temperature of the virtual particle were set as 20,000 amu and 10,000 K, respectively. Since d-AFED allows these parameters to be increased indefinitely, as long as they are sufficiently higher than those of the physical particles, the simulations will run properly.

A soft harmonic barrier was implemented using a constraint on the system to keep the CV within $\pm$6.5 Å, the approximate bounds of the cages. The word "soft" indicates that the particles can slightly cross the barrier but will be pushed back before they stretch too far out, almost as if an elastic sheet is covering the walls of the cages.

A python algorithm was written to take the histogram with bin widths of 0.1 Å and calculate the mean force in each bin.

After taking the averages, the negative integral of the mean force was taken using a iterative python algorithm to obtain the preliminary free energy profile. The midpoint rectangular approximation method was employed for this numeral integration.

Since the two clathrate cages in this study are roughly identical, in order to obtain more accurate results and average out the error in each side, the free energy profile was made symmetrical. By taking the average of the free energy values at each $\pm q_c$ and setting that as the new free energy at those two points, the free energy profiles were made symmetrical across the axis of $q_c = q_c^{\ddagger}$, where $q_c^{\ddagger}$ represents q_c at the transition state.

Also, since free energy is a change rather than an exact value, the graph can be shifted up or down for convenience. In the case of this study, each graph was shifted so that the absolute minimum touches $q_c = 0$. This was achieved by finding the minimum free energy and subtracting that value from each free energy point.

The free energy profiles from flexible cage simulations were obtained from a prior study using similar methods and the same temperature parameters.[27] The rates in this prior study, however, used a slightly different method for obtaining rates. To make the comparison in the results more valid, all of the rates, in both the rigid and flexible cage cases, were calculated using the same QTST rigid rate coefficient equations (see eqns. 6 & 7).

3 Results / Analysis

The results of simulation were very consistent with past studies and the hypothesis. Figure 4 demonstrates how the free energy profile changes with temperature. It becomes clear from this graph that the free energy at the transition state decreases with temperature.[27] Although this result agrees with prior studies, the exact explanation is tricky and not fully understood. To demonstrate why this is, consider the Helmholtz free energy dependence on temperature:

$$A(T) = U(T) + TS(T). \tag{10}$$

U, the internal energy, and S, the entropy, can both be dependent on temperature. As temperature decreases, the entropy and internal energy could both increase or decrease. This means that a decrease in free energy could be the result of a change in one or both of these variables, meaning that the free energy itself is not enough to explain what causes it to increase or decrease. However, although it could be an interesting problem to explore in the future, the explanation for this effect is not relevant for understanding the main results of this study.

Another expected result is the flattening of the free energy barrier. As temperature decreases, the quantum probability distribution widens, increasing the possibility of quantum tunneling. At 25 K, this effect begins to become apparent. It is likely that if the simulations were run at lower temperatures, the curves would approach a plateau surrounding the transition state.[27]

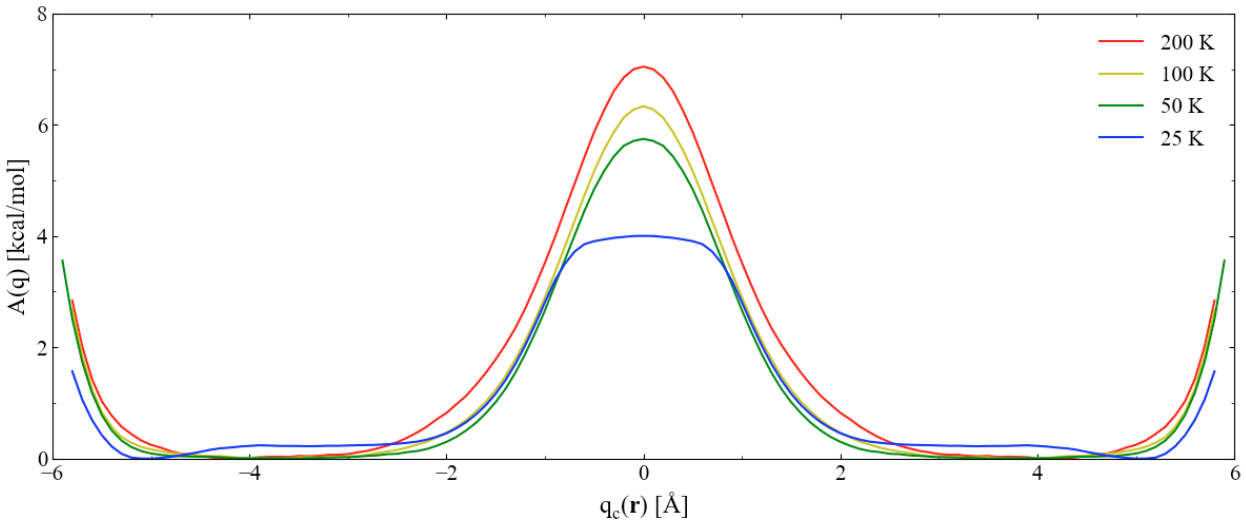

Figure 4. The free energy profile for rigid cage simulations at each of the specified temperature, shifted down for comparison.

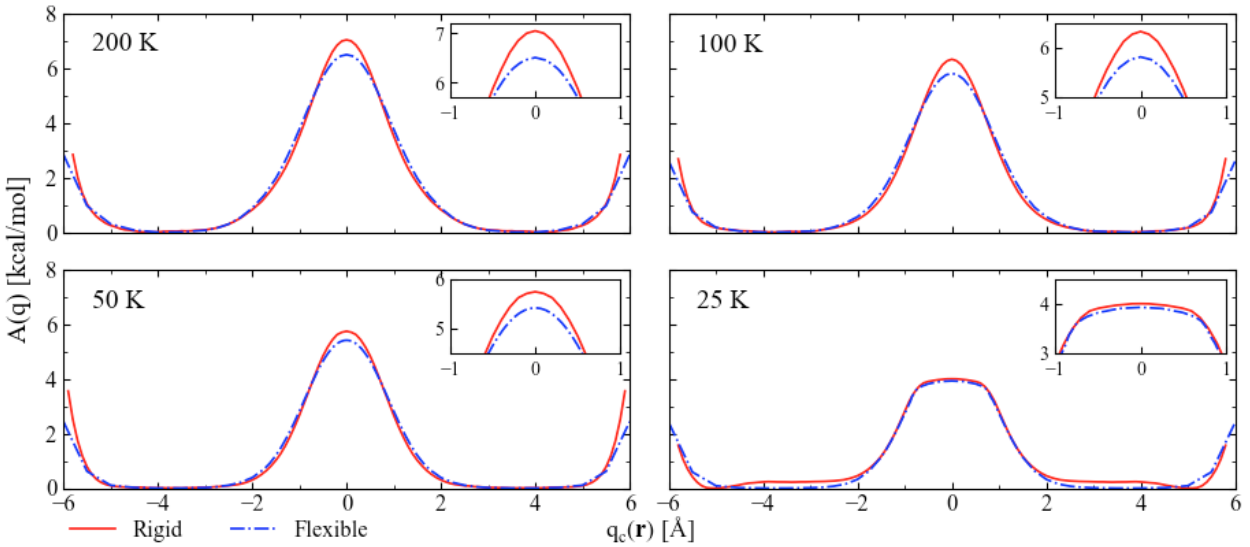

Figure 5. The free energy profile of rigid cage simulations versus flexible cage simulations at each specified temperature. The inset graph in each corner zooms in on the profile near the transition state.

Figure 5 compares the free energy profile of each flexible and rigid cage simulation at each same temperature. As posited previously[27,30] and hypothesized in this study, the flexible cage free energy profiles were higher than those of the rigid cages. This is likely due to the hexagonal face connecting the two cages expanding in the flexible simulations as a result of H_2 pushing against the water molecules. It also makes sense that there was less of a difference between the free energy profiles as temperature decreased, since the average kinetic energy decreased, making the transition state more rigid.

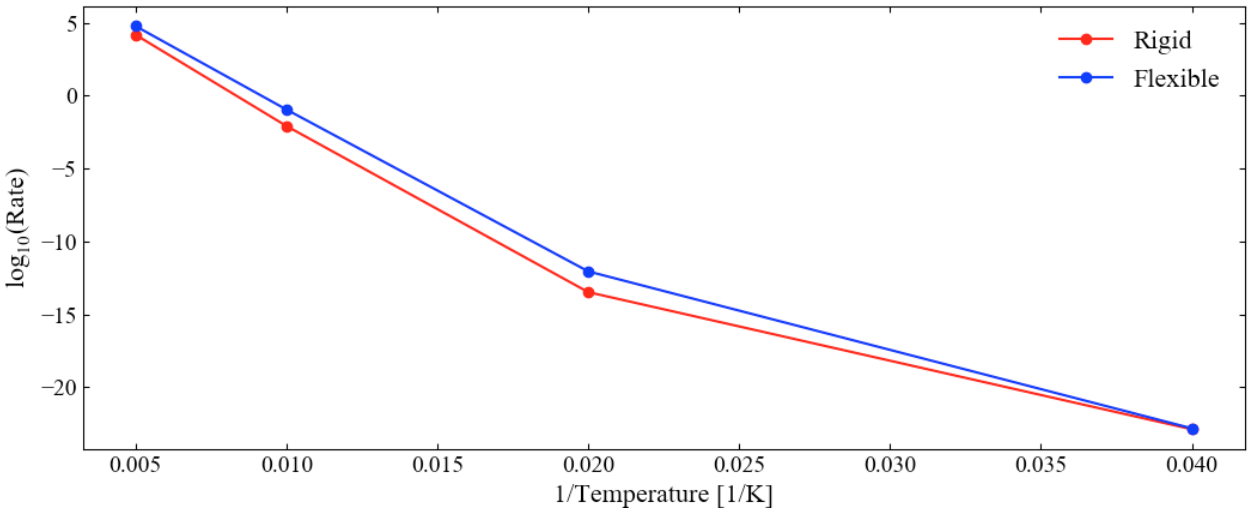

Figure 6. The static quantum rates for both the rigid and flexible cage simulations at 25 K, 50 K, 100 K, and 200 K. The log and inverse scales make the graph linear and thus more view-able.

Additionally, the rates agree with these results (see figure 6). The rates of the flexible simulations are clearly the same or higher at each temperature. This is expected, as a lower free energy profile should result in a higher rate. Also, as with the free energy profiles, the 25 K rates are similar since the flexible cages approximate rigid cages at low temperatures.

Although the graphics demonstrate a difference, the numbers more clearly show that it is significant. The rates of each temperature for each simulation and the factor of increase is shown in table 3.

Table 3. Comparison of the rates from the rigid cage and flexible cage simulations. All rates are in units of [1/s] and all values are rounded to 3 decimal places (the actual values are much more precise).

Temperature	Rigid Rate	Flexible Rate	Factor of Increase
200 K	$1.517 \cdot 10^{4}$	$5.960 \cdot 10^{4}$	$3.928 \cdot 10^{0}$
100 K	$8.343 \cdot 10^{-3}$	$1.124 \cdot 10^{-1}$	$1.348 \cdot 10^{1}$
50 K	$3.327 \cdot 10^{-14}$	$8.921 \cdot 10^{-13}$	$2.648 \cdot 10^{1}$
25 K	$1.319 \cdot 10^{-23}$	$1.523 \cdot 10^{-23}$	$1.155 \cdot 10^{0}$

The numbers indicate that for the higher temperatures, the flexible rates are at least 4 times higher than the rigid rates. While this is not the largest difference, it is still considered significant. But the most interesting result is for the 100 K case. Not only are the flexible cage simulation rates higher by at least 10 fold, but 100 K is close to the temperature range in which the cages are most likely to be stored. A likely cause of this, as described before, is the beads in the 100 K and 50 K cases forming a more ball-like structure, which can expand the transition state in the flexible simulations but cannot do so in the rigid simulations. The smaller difference at 200 K can be attributed to the beads forming a smaller ball, and the smaller difference at 25 K can be attributed to the beads stretching out to form a thin line. Figure 7 shows these bead formations in the rigid simulations, but does not demonstrate the transition state expanding any more or less as a result.

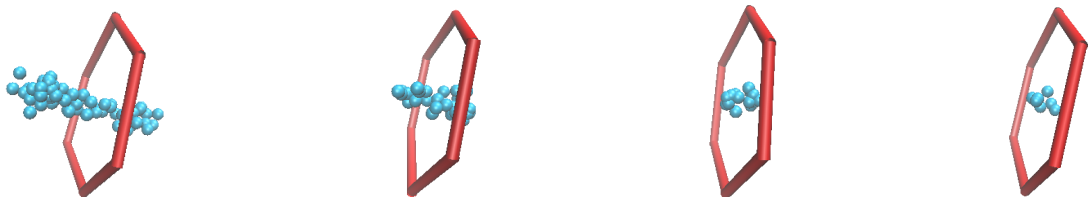

(a) 25K **(b)** 50K **(c)** 100K **(d)** 200K

Figure 7. Visualizations of the beads at the transition state for each temperature (created using VMD).

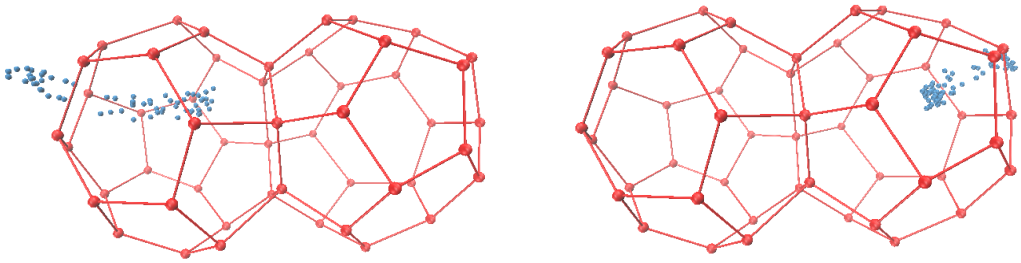

Figure 8. Visualizations of the beads bursting from the sides of the cages (created using VMD).

Another possible reason for the small factor of increase at 25 K could be simulation errors. It is clearly present from the free energy profile at 25 K that the shape around the low free energy zones are not the same shape as the other temperatures. More specifically, they have a clear dimple where in the other graphs the same region is much flatter. Upon analysis of the structure using VMD, it becomes clear why this dimple occurs. The beads of the H_2 atom are supposed to sample the 3-space solely within the two cages. In the 25 K 3-space, however, there are several points at which the beads cross out of one of the cages and into empty space. In the real crystal structure, such movement would be realistic, as most faces within the framework are shared by two cages (except, of course, the faces of the outermost cages). However, in these simulations, only two cages are present, and such movement of the beads will create error in the calculations. Visualizations of these error points are displayed in figure 8.

Luckily, this error had a minute effect on the results, and accounting for it even strengthens them. When the beads diffuse through the wrong face, they are met with a soft wall harmonic barrier, which applies an increasing force in the opposite direction that the particle hits it. This extra force will result in a higher mean force at values of the CV far from the transition state. When the negative integral is taken to obtain the free energy, this should result in a lower free energy at those points. This is exactly reflected in the free energy profile. If these points of the phase space were not sampled, it becomes clear that the dimple in the free energy profile would be pushed up, and the factor of increase between the rates for 25 K would increase.

4 Conclusion

Despite the slight issues, it is without doubt that assuming rigid cages provides significantly different results to that of flexible cages. As a result, simulations in the future will need to include flexibility of the cages as a factor, or else these simulations will not provide accurate data.

The main direction for future clathrate research is to scale up simulations. Although it may be hard to see the place of these results in the grand scheme of things, they are important for the future of clathrate research,

since experts[27] say that sufficiently accurate results will likely only be obtained if the simulation is scaled up. So far, simulation studies have only examined two adjacent clathrate cages. The actual lattice, however, is made up of millions, if not billions. While it is likely not necessary to simulate the entire physical lattice, adding cages will likely affect diffusion rates. The main obstacle to performing these larger-scale simulations is, of course, their computational difficulty. While these studies have yet to be performed, in order to save time, it is crucial that the processes being simulated are fully understood so that certain factors that affect the results do not end up introducing error into these larger-scale simulations. Since flexibility is such a large factor, and not every study so far has included it, this result is crucial to keeping future simulations sufficiently accurate.

Another smaller but still important direction for clathrate research is to study multiple occupancy. The large cages of the sII clathrate hydrate have been shown to hold up to 4 H_2 molecules, and no study so far has examined the effects of multiple occupancy on free energies and diffusion rates. Again, knowing that the cage flexibility plays a role in diffusion, these future simulations will now be much more accurate.

In summary, experts want to increase the scale of simulation in the future, and this study provides the tools to accomplish it. I have proven that without taking flexibility of the cages into account, the results will be inaccurate, making the goal of creating a marketable product impossible to reach. My methodology and conclusions will directly lead to future data which can prove the value of clathrate hydrates to companies that are willing and able to produce them in large quantities. In the long run, this will help to expand the market of renewable energy sources and replace that of fossil fuels, bringing society toward a clean and sustainable future.

References

1. Union of Concerned Scientists, "The Hidden Costs of Fossil Fuels," August 30, 2016. [Online]. Available: https://www.ucsusa.org/clean-energy/coal-and-other-fossil-fuels/hidden-cost-of-fossils.

2. Kerschner, C., Prell, C., Feng, K. & Hubacek, K. Economic vulnerability to peak oil. *Glob. Environ. Chang.* **23**, 1424–1433, DOI: https://doi.org/10.1016/j.gloenvcha.2013.08.015 (2013).

3. Brandt, A. R., M.-Ball, A., Ganser, M. & Gorelick, S. M. Peak oil demand: The role of fuel efficiency and alternative fuels in a global oil production decline. *Environ. Sci. Technol.* **47**, 8031–8041, DOI: https://doi.org/10.1021/es401419t (2013).

4. Intergovernmental Panel on Climate Change (IPCC), "Climate Change 2014 Synthesis Report Summary for Policymakers," 2014. [Online]. Available: http://ipcc.ch/pdf/assessment-report/ar5/syr/AR5_SYR_FINAL_SPM.pdf.

5. Epstein, P. R. *et al.* Full cost accounting for the life cycle of coal. *Ann. N.Y. Acad. Sci.* **1219**, 73–98, DOI: https://doi.org/10.1111/j.1749-6632.2010.05890.x (2011).

6. Environmental Protection Agency (EPA). "Air pollution emissions trends data," Washington, DC, 2016. [Online]. Available: https://www.epa.gov/air-emissions-inventories/air-pollutant-emissions-trends-data.

7. Environmental Protection Agency (EPA), "Nitrogen oxides (NOx) control regulations," Washington, DC, 2016. [Online]. Available: http://www.epa.gov/region1/airquality/nox.html.

8. Environmental Protection Agency (EPA), "Acid rain," Washington, DC, 2016. [Online]. Available: http://www.epa.gov/acidrain/.

9. State of Global Air, "Trends in the global health burden from outdoor air pollution." Accessed October 28, 2018. [Online]. Available: https://www.stateofglobalair.org/health/trends.

10. Agency for Toxic Substances and Disease Registry (ATSDR), "Toxicological profile for Plutonium," January 21, 2015. [Online]. Available: https://www.atsdr.cdc.gov/phs/phs.asp?id=646&tid=119.

11. Beckjord, E. S. *et al.* "The Future of Nuclear Power AN INTERDISCIPLINARY MIT STUDY," [Online]. Available: https://web.mit.edu/nuclearpower/pdf/nuclearpower-full.pdf.

12. Taebi, B. The morally desirable option for nuclear power production. *Philos. Technol.* **24**, 169–192, DOI: https://doi.org/10.1007/s13347-011-0022-y (2011).

13. Carley, S., Davies, L. L., Spence, D. B. & Zirogiannis, N. Empirical evaluation of the stringency and design of renewable portfolio standards. *Nat. Energy* **3**, 754–763, DOI: https://doi.org/10.1038/s41560-018-0202-4 (2018).

14. Science Daily, "Managing renewable energy intelligently," March 25, 2014. [Online]. Available: www.sciencedaily.com/releases/2014/03/140325094814.htm.

15. Zheng, W. *et al.* Durable and self-hydrating tungsten carbide-based composite polymer electrolyte membrane fuel cells. *Nat. Commun.* **8**, 418, DOI: https://doi.org/10.1038/s41467-017-00507-6 (2017).

16. Zhu, M. *et al.* Metal-free photocatalyst for h2 evolution in visible to near-infrared region: Black phosphorus/graphitic carbon nitride. *J. Am. Chem. Soc.* **139**, 13234–13242, DOI: https://doi.org/10.1021/jacs.7b08416 (2017).

17. Guo, L. *et al.* MoS_2/TiO_2 heterostructures as nonmetal plasmonic photocatalysts for highly efficient hydrogen evolution. *Energy Environ. Sci.* **11**, 106–114, DOI: https://doi.org/10.1039/C7EE02464A (2018).

18. Bockris, J. O. Energy, the solar-hydrogen alternative. *Int. J. Energy Res.* **1**, 369–369, DOI: https://doi.org/10.1002/er.4440010409 (1977).

19. Züttel, A. Hydrogen storage methods. *Naturwissenschaften* **91**, 157–172, DOI: https://doi.org/10.1007/s00114-004-0516-x (2004).

20. *Fire Protection Guide to Hazardous Materials, 2010 Edition*, National Fire Protection Association, 2010.

21. Universal Industrial Gases, Inc., *Material Safety Data Sheet Gaseous Hydrogen*, MSDS H2-G, 2015. [Online]. Available: http://www.uigi.com/MSDS_gaseous_H2.html.

22. Environmental Protection Agency (EPA), "Safety and Security Analysis: Investigative Report by NASA on Proposed EPA Hydrogen-Powered Vehicle Fueling Station," Rep. EPA420-R-04-016, 2004. [Online]. Available: https://archive.epa.gov/otaq/fuelcell/web/pdf/420r04016.pdf.

23. Struzhkin, V. V., Militzer, B., Mao, W. L., Mao, H.-K. & Hemley, R. J. Hydrogen storage in molecular clathrates. *Chem. Rev.* **107**, 4133–4151, DOI: https://doi.org/10.1021/cr050183d (2007).

24. Sloan, E. D. & Koh, C. A. *Clathrate Hydrates of Natural Gases* (CRC Press, Taylor and Francis Group, Boca Raton, FL, 2008).

25. Mao, W. L. *et al.* Hydrogen clusters in clathrate hydrate. *Science* **297**, 2247–2249, DOI: https://doi.org/10.1126/science.1075394 (2002).

26. DOE. https://www.energy.gov/eere/fuelcells/doe-technical-targets-onboard-hydrogen-storage-light-duty-vehicles, the targets for future hydrogen storage economy as defined by the Department of Energy.

27. Cendagorta, J. R. *et al.* Competing quantum effects in the free energy profiles and diffusion rates of hydrogen and deuterium molecules through clathrate hydrates. *Phys. Chem. Chem. Phys.* **18**, 32169–32177, DOI: http://dx.doi.org/10.1039/C6CP05968F (2016).

28. Mao, W. L. & Mao, H.-K. Hydrogen storage in molecular compounds. *Proc. Natl. Acad. Sci. USA* **101**, 708–710, DOI: https://doi.org/10.1073/pnas.0307449100 (2004).

29. Vos, W. L., Finger, L. W., Hemley, R. J. & Mao, H.-K. Pressure dependence of hydrogen bonding in a novel H_2O - H_2 clathrate. *Chem. Phys. Lett.* **257**, 524–530, DOI: https://doi.org/10.1016/0009-2614(96)00583-0 (1996).

30. Trinh, T. T., Waage, M. H., van Erp, T. S. & Kjelstrup, S. Low barriers for hydrogen diffusion in sii clathrate. *Phys. Chem. Chem. Phys.* **17**, 13808–13812, DOI: https://doi.org/10.1039/C5CP01713K (2015).

31. Alavi, S., Ripmeester, J. A. & Klug, D. D. Molecular-dynamics study of structure ii hydrogen clathrates. *J. Chem. Phys.* **123**, 024507, DOI: https://doi.org/10.1063/1.1953577 (2005).

32. Alavi, S. & Ripmeester, J. A. Hydrogen-gas migration through clathrate hydrate cages. *Angew. Chem.* **46**, 8933–8933, DOI: https://doi.org/10.1002/anie.200700250 (2007).

33. Senadheera, L. & Conradi, M. S. Rotation and diffusion of H_2 in hydrogen-ice clathrate by h nmr. *J. Phys. Chem. B* **111**, 12097–12102, DOI: https://doi.org/10.1021/jp074517+ (2007).

34. Okuchi, T., Moudrakovski, I. L. & Ripmeester, J. A. Efficient storage of hydrogen fuel into leaky cages of clathrate hydrate. *Appl. Phys. Lett.* **91**, 171903, DOI: https://doi.org/10.1063/1.2802041 (2007).

35. Yoshioka, H. *et al.* Decomposition kinetics and recycle of binary hydrogen-tetrahydrofuran clathrate hydrate. *AIChE J.* **57**, 265–272, DOI: https://doi.org/10.1002/aic.12241 (2011).

36. Burnham, C. J., Futera, Z. & English, N. J. Quantum and classical inter-cage hopping of hydrogen molecules in clathrate hydrate: temperature and cage-occupation effects. *Phys. Chem. Chem. Phys.* **19**, 717–728, DOI: https://doi.org/10.1039/C6CP06531G (2017).

37. Feynamn, R. P. & Hibbs, A. R. *Quantum Mechanics and Path Integrals* (McGraw-Hill, New York, 1965).

38. Abrams, J. B. & Tuckerman, M. E. Efficient and direct generation of multidimensional free energy surfaces via adiabatic dynamics without coordinate transformations. *J. Phys. Chem. B* **112**, 15742–15757, DOI: https://doi.org/10.1021/jp805039u (2008).

39. Chen, M., Cuendet, M. A. & Tuckerman, M. E. Heating and flooding: A unified approach for rapid generation of free energy surfaces. *J. Chem. Phys.* **137**, 024102, DOI: https://doi.org/10.1063/1.4733389 (2012).

40. Martyna, G. J., Klein, M. L. & Tuckerman, M. E. Nosé–hoover chains: The canonical ensemble via continuous dynamics. *The J. Chem. Phys.* **97**, 2635–2643, DOI: https://doi.org/10.1063/1.463940 (1992).

41. Margul, D. T. & Tuckerman, M. E. A stochastic, resonance-free multiple time-step algorithm for polarizable models that permits very large time steps. *J. Chem. Theory Comput.* **12**, 2170–2180, DOI: https://doi.org/10.1021/acs.jctc.6b00188 (2016).

42. Tuckerman, M. E., Yarne, D. A., Samuelson, S. O., Hughes, A. L. & Martyna, G. J. Exploiting multiple levels of parallelism in molecular dynamics based calculations via modern techniques and software paradigms on distributed memory computers. *Comput. Phys. Commun.* **128**, 333 – 376, DOI: https://doi.org/10.1016/S0010-4655(00)00077-1 (2000).